EVALUATION OF CERTAIN ALGERIAN MEDICINAL PLANT EXTRACTS AS POTENTIAL INHIBITORS OF SARS-COV-2 MAIN PROTEASE (3CLPRO) USING MOLECULAR DOCKING

BENOUNISSA Kadda[1] GHOMRI Amina*[1,2]

[1]Laboratory of Naturals Products and Bioactives- LASNABIO,University of Tlemcen. B. P. 119, 13000 Tlemcen. Algeria.

[2]Ecole Supérieure en Sciences Appliquées de Tlemcen ESSA TlemcenB. P.165 belhorizon 13000 Tlemcen. Algeria.

Received: 15/08/2025

Accepted:10/03/2026

Published: 11/05/2026

Abstract

Molecular modeling has become one of the most widely used computational tools for predicting and reproducing protein–ligand complexes. In this work, we investigated the biological and pharmacological activity of bioactive molecules from five Algerian medicinal plants traditionally used to treat arterial hypertension (Artemisia herba-alba, Myrtus communis, Pinus maritima, Citrus lemon, and Crataegus sp. (Aubépine)). Using molecular docking with the MOE 2015 software and the AMBER10 force field, the active molecules were docked against the main protease of SARS-CoV-2, 3C-like protease (3CLpro, PDB: 6LU7), which plays a critical role in viral replication. Among all ligands tested, Procyanidin B1 (from Pinus maritima) exhibited the best binding score (−8.0157 kcal/mol), outperforming the reference drugs chloroquine and hydroxychloroquine. Several other natural molecules—Myricetin-3-O-rhamnoside, Proanthocyanidins, and siloxane derivatives from Crataegus—also demonstrated superior binding affinity compared to synthetic inhibitors. All tested ligands were shown to be non-toxic. These findings suggest that Pinus maritima, in particular, represents a promising natural source for the development of novel anti-COVID-19 therapeutics.

Keywords: COVID-19, SARS-CoV-2, 3CLpro, Molecular docking, Medicinal plants, Procyanidin B1, Pinus maritima, Arterial hypertension, MOE, Molecular modeling

1. Introduction

The world is currently experiencing an unprecedented health crisis caused by the Severe Acute Respiratory Syndrome Coronavirus-2 (SARS-CoV-2), the causative agent of Coronavirus Disease 2019 (COVID-19). First reported in Wuhan, Hubei Province, China on December 31, 2019, the virus rapidly spread globally, prompting the World Health Organization (WHO) to declare a pandemic on March 11, 2020. By March 2021, the pandemic had resulted in over 120 million confirmed cases and more than 2.6 million deaths worldwide [1].

Clinical reports have highlighted hypertension (30%), diabetes (19%), and coronary artery disease (8%) as the most prevalent comorbidities among COVID-19 patients, correlating with increased disease severity and mortality [2]. The mechanistic link between hypertension and COVID-19 severity involves the angiotensin-converting enzyme 2 (ACE2), which SARS-CoV-2 exploits as a cellular entry receptor [3]. Hypertensive patients treated with ACE inhibitors or angiotensin receptor blockers (ARBs) exhibit higher ACE2 expression, potentially increasing susceptibility to infection [4].

Medicinal plants represent a rich source of biologically active compounds that have served as the foundation for drug discovery throughout history [5]. Algeria harbors exceptional botanical diversity, with numerous plants traditionally employed in folk medicine to treat hypertension and cardiovascular conditions. Given the absence of specific approved treatments for COVID-19 during the studied period and the link between hypertension and COVID-19 severity, we hypothesized that bioactive molecules from Algerian antihypertensive plants might also exhibit inhibitory activity against key SARS-CoV-2 enzymes.

The 3C-like protease (3CLpro), also known as the main protease (Mpro), is an essential enzyme for SARS-CoV-2 replication. It cleaves the viral polyprotein at multiple sites, making it an attractive drug target [6].

Molecular docking is now a cornerstone of modern drug discovery, empowered by advances in computational tools, scoring functions, and docking algorithms that enable accurate prediction of ligand–protein binding [7-9].

This study aims to evaluate, through molecular docking, the inhibitory potential of bioactive molecules from five Algerian medicinal plants against 3CLpro, and to compare their binding affinities with those of the synthetic inhibitors chloroquine and hydroxychloroquine [10].

2. Algerian Medicinal Plants: Antihypertensive Activity

Algeria's flora is particularly rich in medicinal plants used in traditional medicine across the country. The following five plants, widely employed as natural antihypertensive remedies, were selected for this study:

Group	Family	Scientific Name	Vernacular Name	Part Used	Preparation	Region
Dicotyledons	Asteraceae	Artemisia herba-alba Asso	Chih	Flowers & Leaves	Infusion	Dry regions: Mediterranean basin, southern Africa
Myrtales	Myrtaceae	Myrtus communis	Raihen	Leaves	Decoction	Mediterranean regions
Sapindales	Rutaceae	Citrus lemon	L-hamed	Fruit	Juice	Northern Algeria, irrigable zones
Dicotyledons	Rosaceae	Crataegus (Aubépine)	Zaarour lbari	Fruit & Flowers	Infusion	Common throughout Algeria, Atlas forests
Pinales	Pinaceae	Pinus pinaster/maritima	Pin maritime	Bark	Infusion	Atlantic and Mediterranean coast

Table 1. Algerian medicinal plants with antihypertensive activity selected for this study.

The plants below are illustrated showing representative specimens:



Figure 1a. Artemisia herba-alba (Chih) — used as infusion from flowers and leaves.



Figure 1b. Myrtus communis (Raihen) — leaves used in decoction.



Figure 1c. Citrus lemon (L-hamed) — fruit juice used.



Figure 1d. Crataegus sp. (Zaarour lbari) — fruits and flowers in infusion.



Figure 1e. Pinus pinaster/maritima (Pin maritime) — bark used in infusion.

3. Materials and Methods

3.1 Enzyme Target: 3C-like Protease (3CLpro)

The crystal structure of SARS-CoV-2 main protease (3CLpro, PDB code: 6LU7) was retrieved from the Protein Data Bank (www.rcsb.org/pdb). This enzyme (classification: Viral Protein;

expression system: E. coli BL21(DE3); X-ray diffraction resolution: 2.16 Å; chain: A) plays a critical role in the processing of viral polyproteins and represents an ideal drug target due to its absence in human cells.

Parameter	Value
Enzyme	3C-like proteinase (3CLpro)
PDB Code	6LU7
Classification	Viral Protein
Organism	SARS-CoV-2 / synthetic construct
Resolution	2.16 Å
Method	X-Ray Diffraction
Chains	A

Table 2. Crystallographic data for the 3CLpro enzyme (PDB: 6LU7).

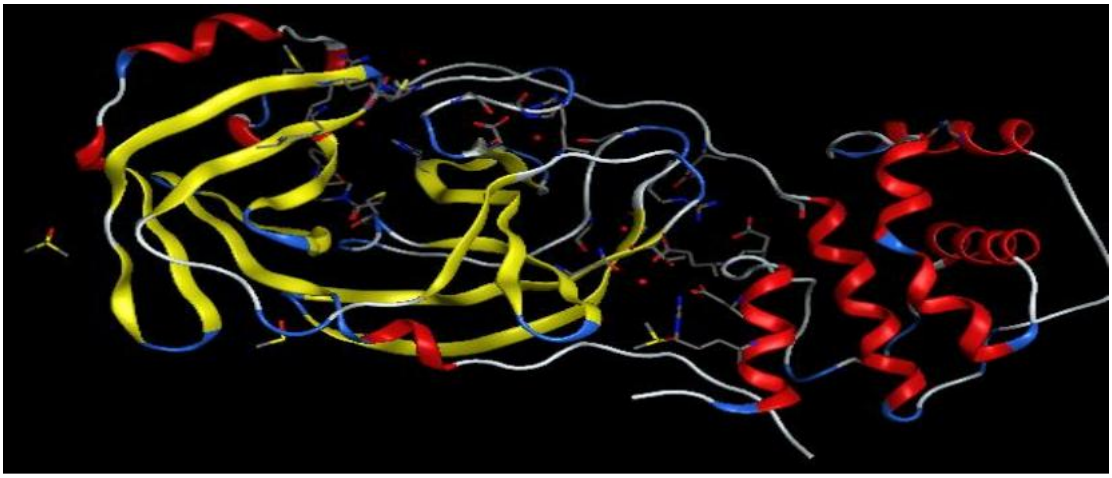


Figure 2. 3D ribbon representation of the downloaded 3CLpro enzyme structure (PDB: 6LU7). Alpha-helices are shown in red, beta-sheets in yellow.

3.2 Active Site Determination

The active site of 3CLpro was identified using the 'Site Finder' module within MOE software, which detects enzymatic cavities based on geometric and physicochemical properties. The primary binding site (Site 1, size = 109, PLB = 2.55, Hyd = 21, Side = 60) contains key residues including THR24, THR25, THR26, LEU27, PHE140, ASN142, GLY143, SER144, CYS145, HIS163, HIS164, MET165, GLU166, and GLN189. (Figure 3)

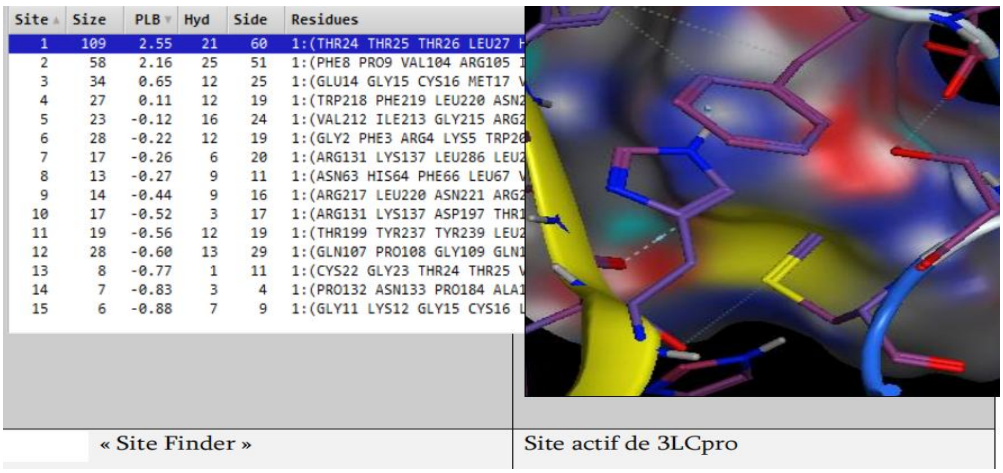


Figure 3. The active site of 3CLpro (PDB: 6LU7).

3.3 Molecular Docking Protocol

All molecular docking calculations were performed using MOE 2015 (Molecular Operating Environment) software, employing the AMBER10:EHT force field. The docking protocol consisted of: (1) preparation and minimization of the enzyme structure, including removal of water molecules and co-crystallization molecules; (2) semi-empirical EHT optimization of all ligand structures; (3) molecular docking of each ligand into the active site; and (4) scoring and ranking of binding poses based on docking score (S, kcal/mol) and RMSD values [15].

The reference ligand (co-crystallized inhibitor of 6LU7) was re-docked to validate the protocol. A pose was selected as valid if RMSD < 2.0 Å compared to the crystallographic pose. Synthetic inhibitors chloroquine (CID: 2719) and hydroxychloroquine (CID: 3652) were used as reference compounds for comparison with natural ligands. (figures 4a, 4b)

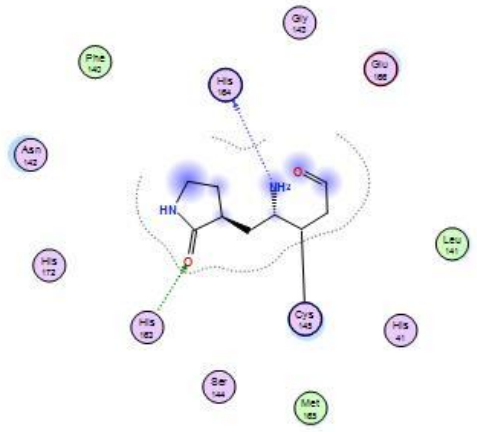


Figure 4a. RMSD values obtained for reference ligand re-docking runs against 3CLpro (6LU7). The best pose (RMSD = 1.5928 Å) confirms docking protocol validity.

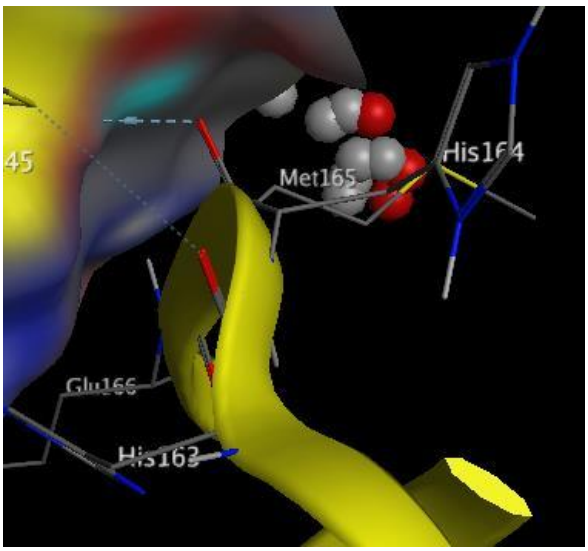


Figure 4b. 3D visualization of the validated reference ligand pose within the 3CLpro active site.

3.4 Selected Natural Ligands

Based on literature review, bioactive molecules were identified for each plant and downloaded from the PubChem database (pubchem.ncbi.nlm.nih.gov) in PDB format. The selected molecules are summarized in the table below.

Plant	Selected Bioactive Molecules	References
Artemisia herba-alba	Camphor, Camphene, Chrysanthenone, Borneol, 1,8-Cineol	[11]
Myrtus communis	Ethyl acetate, Myricetin-3-O-rhamnoside	[12]
Pinus maritima	Catechin, Epicatechin, Taxifolin, Procyanidins/Proanthocyanidins, Flavan-3-ols, Procyanidin B1, Caffeic acid, Ferulic acid, p-Hydroxybenzoic acid	[14]
Citrus lemon	Limonene, Neral, β-Pinene, γ-Terpinene, β-Myrcene	[5]
Crataegus sp. (Aubépine)	Tetradecamethylcycloheptasiloxane, Mandelic acid, Dodecamethylcyclohexasiloxane, Decamethylcyclopentasiloxane, 3-Isopropoxy-hexamethyl-tris(trimethylsiloxy)tetrasiloxane	[13]

Table 3. Bioactive molecules selected from each medicinal plant for molecular docking against 3CLpro.

4. Results and Discussion

4.1 Toxicity and Physicochemical Properties

Toxicity predictions and physicochemical properties of all ligands were computed using MOE software. None of the tested molecules exhibited predicted toxicity, confirming their safety profile for further investigation. Key parameters including molecular weight, TPSA (Topological Polar Surface Area), H-bond donors/acceptors, and logP values are summarized below for representative compounds.

Ligand	MW (g/mol)	TPSA (Å²)	H-don	H-acc	logP	logS	Toxic
1,8-Cineol	154.25	9.23	0	1	2.74	-1.90	No
Camphor	152.24	17.07	0	1	2.40	-2.09	No
Myricetin-3-O-rhamnoside	464.38	206.60	8	11	0.22	-2.72	No
Catechin	290.27	110.38	5	6	1.64	-1.74	No
Taxifolin	304.25	127.45	5	7	1.28	-2.01	No
Procyanidin B1	592.55	209.76	9	12	3.49	-4.14	No
Proanthocyanidins	592.55	209.76	9	12	3.49	-4.14	No
Limonene	136.24	0.00	0	0	3.31	-3.01	No

Table 4. Physicochemical properties and toxicity predictions for selected ligands (computed with MOE).

4.2 Molecular Docking Scores

The molecular docking results for all ligands against the 3CLpro active site are presented in Table 5. The docking score (S, kcal/mol) reflects binding affinity, with more negative values indicating stronger binding. The RMSD value indicates the deviation between the initial and final ligand pose after refinement.

Ligand	Plant/Source	Score S (kcal/mol)	RMSD (Å)	Best?
Reference Ligand (6LU7)	—	-5.2091	1.5928	Ref
Chloroquine	Synthetic	-6.5155	0.9806	
Hydroxychloroquine	Synthetic	-6.9297	0.9643	
1,8-Cineol	Artemisia herba-alba	-4.6912	1.5727	

Camphor	Artemisia herba-alba	-4.5834	0.8404	
Chrysanthenone	Artemisia herba-alba	-4.4375	1.6389	
Borneol	Artemisia herba-alba	-4.6037	1.8398	
Myricetin-3-O-rhamnoside	Myrtus communis	-7.6035	1.5371	★
Catechin	Pinus maritima	-6.1578	0.7870	
Epicatechin	Pinus maritima	-6.1910	0.9939	
Taxifolin	Pinus maritima	-6.1455	1.2236	
Proanthocyanidins	Pinus maritima	-7.5597	2.5515	★
Flavan-3-ols	Pinus maritima	-5.9101	1.8630	
Procyanidin B1	Pinus maritima	-8.0157	1.7189	★★
Caffeic acid	Pinus maritima	-4.9407	0.6495	
Ferulic acid	Pinus maritima	-5.0970	1.2830	
Limonene	Citrus lemon	-4.7080	2.3313	
β-Pinene	Citrus lemon	-4.5393	2.1057	
γ-Terpinene	Citrus lemon	-4.9624	1.3281	
Tetradecamethylcycloheptasiloxane	Crataegus sp.	-7.4339	1.6875	★
Dodecamethylcyclohexasiloxane	Crataegus sp.	-6.2099	1.6546	
Decamethylcyclopentasiloxane	Crataegus sp.	-6.1239	2.1292	
3-Isopropoxy-hexamethyl-tris(TMS)-tetrasiloxane	Crataegus sp.	-7.5741	1.7415	★

Table 5. Molecular docking results for all ligands against 3CLpro (6LU7). ★ = score better than chloroquine/hydroxychloroquine; ★★ = best overall score.

4.3 Interaction Analysis

The reference ligand formed a total of 30 interactions with key residues of the 3CLpro active site, including 6 hydrogen-donor interactions, 7 ionic interactions, 10 hydrogen-acceptor interactions, 6 H-Pi interactions, and 1 Pi-Pi interaction. Key interacting residues included HIS41, CYS145, MET49, ASN142, GLN189, GLU166, and HIS164—residues known to be critical for substrate binding.

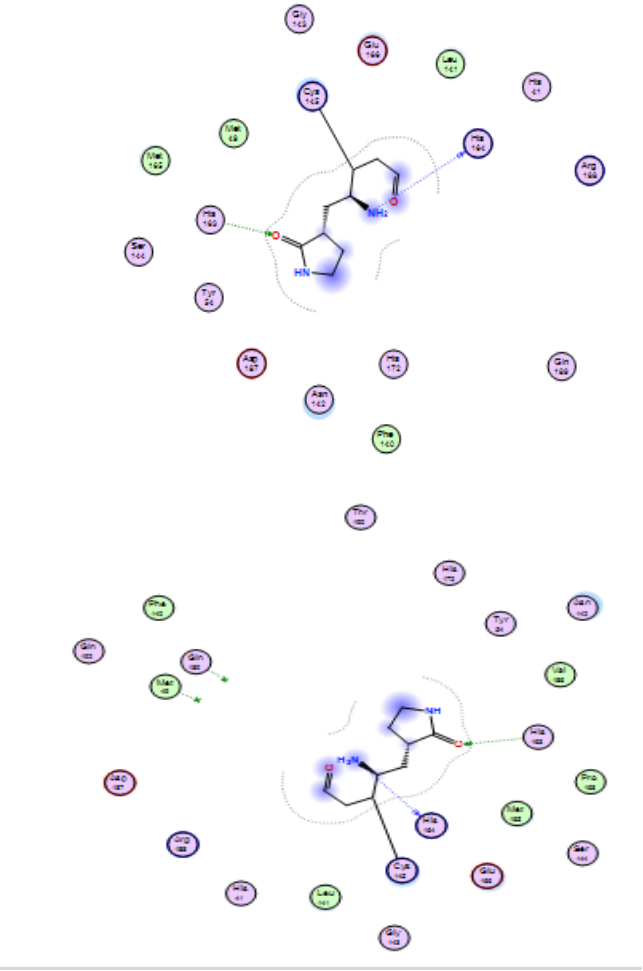


Figure 5. 2D (left) and 3D (right) interaction diagrams between 3CLpro and the reference ligand/Myricetin-3-O-rhamnoside. The reference ligand engages multiple hydrogen-bond donor and acceptor interactions with catalytic residues.

6LU7: VIRAL PROTEIN / 6LU7: VIRAL PROTEIN

Ligand		Receptor				Interaction	Distance	E (kcal/mol)
N5	24	O	HIS	164	(A)	H-donor	3.07	-0.9
O8	23	NE2	HIS	163	(A)	H-acceptor	2.52	-0.9

6LU7: VIRAL PROTEIN / 6LU7

Ligand		Receptor				Interaction	Distance	E (kcal/mol)
C	21	SD	MET	49	(A)	H-donor	3.84	-0.7
O	1	NE2	GLN	189	(A)	H-acceptor	2.86	-2.8

Figure 6. Summary of key interactions between Myricetin-3-O-rhamnoside and the 3CLpro active site. H-donor interactions with HIS164 (3.07 Å, −0.9 kcal/mol) and H-acceptor with MET49 are shown.

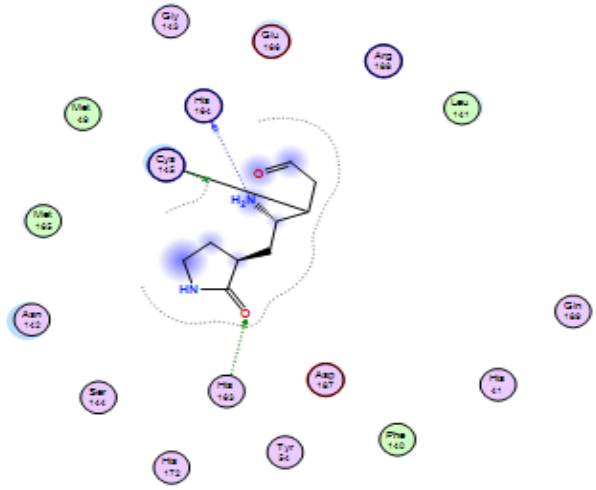


Figure 7. 2D and 3D interaction diagrams of Taxifolin with 3CLpro. Key contacts with HIS41, CYS145, HIS163, HIS164, PHE140, and LEU27 are highlighted in the 3D view.

6LU7: VIRAL PROTEIN / 6LU7: VIRAL PROTEIN

Ligand		Receptor				Interaction	Distance	E (kcal/mol)
N5	24	O	HIS	164	(A)	H-donor	3.07	-0.9
O8	23	NE2	HIS	163	(A)	H-acceptor	2.52	-0.9

6LU7: VIRAL PROTEIN / 6LU7

Ligand		Receptor				Interaction	Distance	E (kcal/mol)
O	4	N	CYS	145	(A)	H-acceptor	3.06	-1.7
O	4	SG	CYS	145	(A)	ionic	3.09	-3.9

6LU7: VIRAL PROTEIN / 6LU7

Figure 8. Interaction report for Taxifolin: H-acceptor with CYS145 N (3.06 Å, −1.7 kcal/mol) and ionic interaction with CYS145 SG (3.09 Å, −3.9 kcal/mol).

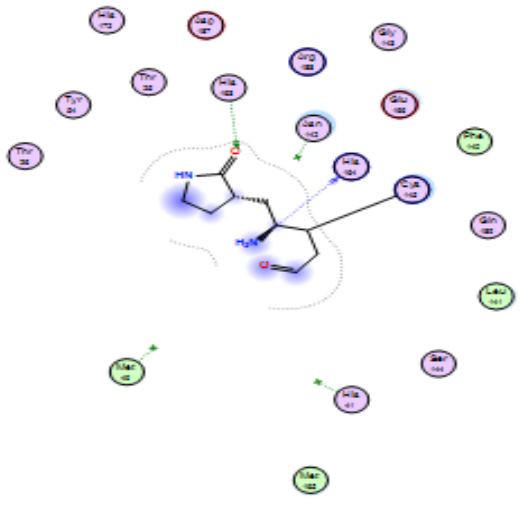


Figure 9. 2D and 3D interaction diagrams of Proanthocyanidins with 3CLpro, showing key contact with MET49.

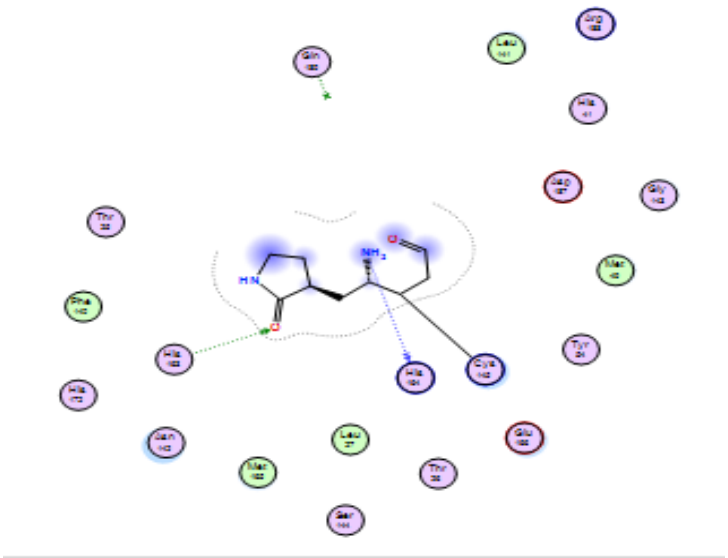


Figure 10. 2D interaction diagram for Procyanidin B1 — the best-performing natural ligand (score: −8.0157 kcal/mol) — showing extensive interactions within the 3CLpro active site.

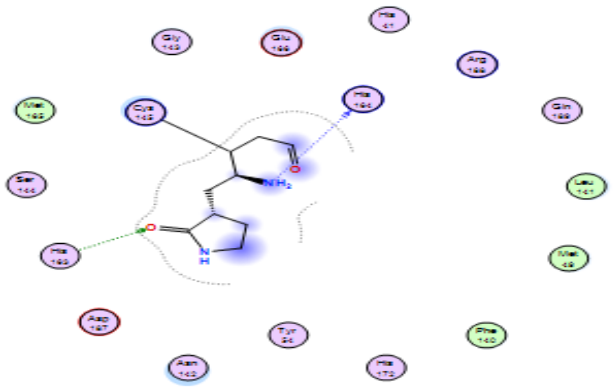


Figure 11. Interaction report for Procyanidin B1: H-donor with HIS164 (3.07 Å), H-acceptor with HIS163 (2.52 Å), and Pi-H interaction with GLN189 (3.93 Å, −1.7 kcal/mol).

6LU7: VIRAL PROTEIN / 6LU7: VIRAL PROTEIN

Ligand	Receptor				Interaction	Distance	E (kcal/mol)
N5 24	O	HIS	164	(A)	H-donor	3.07	-0.9
O8 23	NE2	HIS	163	(A)	H-acceptor	2.52	-0.9

6LU7: VIRAL PROTEIN / 6LU7

Ligand	Receptor				Interaction	Distance	E (kcal/mol)
O 10	NE2	GLN	189	(A)	H-acceptor	2.79	-3.2

Figure 12. Interaction report for 3-Isopropoxy-hexamethyl-tris(trimethylsiloxy)tetrasiloxane (from Crataegus): H-donor with HIS164, H-acceptor with HIS163 and GLN189 (2.79 Å, −3.2 kcal/mol).

4.4 Comparison with Synthetic Inhibitors

The most notable finding of this study is that five natural ligands from Algerian medicinal plants surpassed both synthetic inhibitors (chloroquine: −6.5155 kcal/mol; hydroxychloroquine: −6.9297 kcal/mol) in binding affinity against 3CLpro:

Compound	Source	Score (kcal/mol)
Procyanidin B1 ★★ BEST	Pinus maritima	-8.0157
Myricetin-3-O-rhamnoside	Myrtus communis	-7.6035
3-Iso-hexamethyl-tris(TMS)tetrasiloxane	Crataegus sp.	-7.5741
Proanthocyanidins	Pinus maritima	-7.5597
Tetradecamethylcycloheptasiloxane	Crataegus sp.	-7.4339
Hydroxychloroquine (reference drug)	Synthetic	-6.9297
Chloroquine (reference drug)	Synthetic	-6.5155

Table 6. Top-performing natural ligands vs. synthetic inhibitors against 3CLpro.

Procyanidin B1, a proanthocyanidin dimeric compound abundant in pine bark (Pinus maritima), demonstrated the highest binding affinity among all tested ligands. Its superior score (−8.0157 kcal/mol) compared to the reference drug chloroquine (−6.5155 kcal/mol) and hydroxychloroquine (−6.9297 kcal/mol) represents an improvement of approximately 1.5 to 1.1 kcal/mol respectively, indicating significantly stronger interaction with the 3CLpro active site. Crucially, Pinus maritima is already used in traditional Algerian medicine as an antihypertensive remedy, creating a dual therapeutic relevance for COVID-19 patients who present with comorbid hypertension.

5. Conclusion

This study applied molecular docking to evaluate the potential of bioactive molecules from five Algerian medicinal plants (Artemisia herba-alba, Myrtus communis, Pinus maritima, Citrus lemon, and Crataegus sp.) as inhibitors of the SARS-CoV-2 main protease 3CLpro. The main findings are:

Procyanidin B1 (Pinus maritima) showed the highest binding affinity (−8.0157 kcal/mol), surpassing both chloroquine and hydroxychloroquine.

Myricetin-3-O-rhamnoside (Myrtus communis, −7.6035 kcal/mol), two siloxane derivatives from Crataegus sp. (−7.57 and −7.43 kcal/mol), and Proanthocyanidins (Pinus maritima, −7.56 kcal/mol) also outperformed the synthetic drugs.

All ligands tested were predicted to be non-toxic.

The predominant interaction types observed were H-donor, H-acceptor, and ionic interactions with catalytic residues CYS145, HIS41, GLN189, HIS163, HIS164, MET49, and GLU166.

These in silico findings underscore the dual therapeutic relevance of Pinus maritima—a plant traditionally used against hypertension in Algeria—as a potential source of anti-COVID-19 leads. The results provide a rational basis for further in vitro and in vivo validation of these natural compounds, particularly Procyanidin B1, as novel antiviral therapeutics.

References

[1] Zhu N. et al. A novel coronavirus from patients with pneumonia in China, 2019. N Engl J Med 2020; 382:727–733.

[2] Zhou F. et al. Clinical course and risk factors for mortality of adult inpatients with COVID-19 in Wuhan, China. Lancet. 2020; 395:1054–1062.

[3] Wan Y. et al. Receptor recognition by the novel coronavirus from Wuhan: an analysis based on decade-long structural studies of SARS coronavirus. J Virol 2020; 94:e00127-20.

[4] Hoffmann M. et al. SARS-CoV-2 cell entry depends on ACE2 and TMPRSS2 and is blocked by a clinically proven protease inhibitor. Cell 2020; 181:271–280.

[5] Salim B. et al. Identification of phenolic compounds from nettle as new candidate inhibitors of main enzymes responsible on type-II diabetes. Curr Drug Discov Technol 2020; 17:197–202.

[6] Zhang L. et al. Crystal structure of SARS-CoV-2 main protease provides a basis for design of improved α-ketoamide inhibitors. Science 2020; 368:409–412.

[7] Comparative study of aromatase enzyme inhibition by synthetic and natural ligand: Molecular modeling and conceptual DFT investigation, M Fouzia, M Noureddine, G Amina, G Said, Current Enzyme Inhibition 14 (2), 104-113.

[8] In silico comparison of synthetic and natural molecules bindings with acetylcholinesterase enzyme using molecular docking, F Mesli, S Bouchentouf, A Ghomri, M Noureddine, S Ghalem, J. Adv. Mol. Biol 2, 17-26.

[9] Theoretical Investigation of Some Donepezil-based Derivatives as Dual Inhibitors for beta-Amyloid-and Cholinesterase Enzymes, A Meziane, A Ghomri, S Bouchentouf, M El-Shazly, Journal of Biochemical Technology 12 (2-2021), 48- [10] Wang M. et al. Remdesivir and chloroquine effectively inhibit the recently emerged novel coronavirus (2019-nCoV) in vitro. Cell Res 2020; 30:269–271.

[11] Dahmani-Hamzaoui N., Baaliouamer A. Volatile constituents of Algerian Artemisia herba-alba essential oils. J Essent Oil Res 2015; 27:437–446.

[12] Nassar M.I. et al. Secondary metabolites and bioactivities of Myrtus communis. Pharmacognosy Res 2010; 2:325.

[13] Bechkri S. et al. Composition and biological activities of seeds oils of two Crataegus species growing in Algeria. J Mater Environ Sci 2017; 8:1526–1530.

[14] Bate-Smith E.C. Phytochemistry of proanthocyanidins. Phytochemistry 1975; 14:1107–1113.

[15] Jain A.N. Scoring functions for protein-ligand docking. Curr Protein Pept Sci 2006; 7:407–420.